Free Radical Research, March 2009; 43(3): 241–249

informa
healthcare

Elevated oxidative stress, iron accumulation around microvessels and increased 4-hydroxynonenal immunostaining in zone 1 of the liver acinus in hypercholesterolemic rabbits

WEI-YI ONG[1–3], ANDREW M. JENNER[2,4], NING PAN[2,4], CHOON-NAM ONG[3,5], & BARRY HALLIWELL[2,4]

[1]*Department of Anatomy,* [2]*Ageing/Neurobiology and* [3] *Toxicology Research Programmes,* [4]*Department of Biochemistry, and* [5]*Department of Community, Occupational and Family Medicine, National University of Singapore, Singapore 119260*

(Received 13 September 2008; in revised form 12 December 2008)

Abstract
Rabbits were fed a diet containing 1% cholesterol for 8 weeks and the levels of iron and oxidized lipids in liver analysed using atomic absorption spectroscopy and gas chromatography-mass spectrometry. A non-significant trend to an increase in iron level, but significant increases in the lipid peroxidation products, F_2-isoprostanes and the cholesterol oxidation products 7 beta hydroxycholesterol, 7 ketocholesterol and cholesterol 5,6-alpha epoxide were detected in the liver of the cholesterol-fed rabbits. Histological analysis showed greater accumulation of lipids by Sudan red labelling in hepatocytes of zone I than zones II and III of the liver acinus. The increase in lipids coincided with an increase in iron staining in macrophages around liver microvessels and increased immunostaining to melanotransferrin and the lipid peroxidation product, 4-hydroxynonenal (4-HNE), in zone 1. The results are suggestive of microvascular damage associated with iron accumulation and oxidative stress in the liver during hypercholesterolemia.

Keywords: *Hypercholesterolemia, iron, perilobular vessels, liver acinus, oxidative stress, 4-hydroxynonenal, cholesterol oxidation products, oxysterols*

Abbreviations: *AAS, atomic absorption spectrometer; GC-MS, gas chromatography-mass spectrometry; BHT, butylated hydroxytoluene; COPs, cholesterol oxidation products; DAB, 3,3,-diaminobenzidine tetrahydrochloride; DMT1, divalent metal transporter-1; 4-HNE, 4-hydroxynonenal; PBS, phosphate buffered saline; TBS, Tris buffered saline*

Introduction

Reactive oxygen and nitrogen species are widely thought to play an important role in the development of atherosclerosis. Activation of macrophages or their monocyte precursors could generate these species in vessel walls, leading to damage to endothelial and smooth muscle cells [1]. Iron could play a role in the process of atherogenesis through the induction of the formation of oxidized LDL. Macrophage-derived foam cells of human atheromas are rich in iron and ferritin [2,3] and supplementation with iron dextran has been reported to augment the development of atherosclerotic lesions in cholesterol-fed rabbits [4]. Conversely, the iron chelator desferrioxamine inhibits atherosclerotic lesion development and decreases lesion iron concentrations [5]. Furthermore, zinc supplementation decreases iron levels, lipid peroxidation and the development of atherosclerosis in rabbits fed with a high cholesterol diet [6]. The results in hypercholesterolemic rabbits are consistent with those in apoE-deficient mice. These showed iron deposits in atherosclerotic lesions and tissue sections

Correspondence: Dr Wei-Yi Ong, Neurobiology Research Programme, Centre for Life Sciences, National University of Singapore, Singapore 119260. Tel: +65 6516 3662. Fax: +65 6777 3271. Email: antongwy@nus.edu.sg

ISSN 1071-5762 print/ISSN 1029-2470 online
DOI: 10.1080/10715760802691455

of heart and liver in an age-dependent manner, but apoE-deficient mice fed a low-iron diet had smaller lesions than control littermates [7].

Hypercholesterolemia may damage organs other than the vascular system. Our studies on the cerebral cortex of hypercholesterolemic rabbits showed increases in iron near microvessels in the cerebral cortex and subcortical white matter [8]. This suggests that microvascular damage and iron efflux could predispose to oxidative stress in the brain after hypercholesterolemia [9]. A link between a vessel's susceptibility to atherosclerotic lesions and the number of vasa vasorum in the vessel has been demonstrated [10,11]. It was proposed that microvessels could be a source of disease progression in atherosclerosis, due to endothelial impairment, and as a pathway for monocytic cells to migrate to sites of disease [12]. The present study was carried out in view of this possibility, to elucidate a possible connection between microvessel damage and iron-induced oxidative stress in the liver of cholesterol-fed rabbits.

Materials and methods

Rabbits and treatment

New Zealand white rabbits (2–2.5 kg) were fed for 8 weeks with a normal diet (GPR diet, Glen Forrest Stockfeeders, Western Australia, $n = 5$) or a high cholesterol diet (GPR + 1% cholesterol, $n = 7$). Blood samples were obtained for iron and lipid analysis at 0, 4 and 8 weeks after the start of the high cholesterol diet, for the cholesterol-fed rabbits. Samples were obtained at equivalent times from rabbits fed with normal diet. Approximately 3 ml of blood was obtained from the ear veins of rabbits that had been fasted overnight and collected in 6 ml BD Vacutainer® Serum™ Tubes with Clot activator and silicone-coated interior (Ref: 367815, Franklin Lakes, NJ). The whole blood was centrifuged and serum samples transferred to new vials and kept in a -20°C freezer until analysis. Rabbits were sacrificed by injection of Nembutal at the end of 8 weeks and liver and other organs removed and immersed in fixative containing 4% paraformaldehyde in 0.1 M phosphate buffer or flash-frozen in liquid nitrogen for measurement of lipids. All procedures were approved by the Institutional Animal Care and Use Committee.

Serum and liver iron analyses

Determinations were performed using a Varian SpectrAA-220G graphite furnace atomic absorption spectrometer (AAS) equipped with a GTA 110 atomizer, programmable sample dispenser and deuterium background correction. Pyrolytically-coated partitioned graphite tubes were used for this work. All reagents used were of high purity analytical grade for trace element analysis and standards were of AAS grade. Serum samples were thawed at 22°C and digested by diluting 110-times with diluent which contains 0.01 M HNO_3 and 0.02% Triton-X 100 (USB Corporation, Cleveland, OH). The digested samples were well-mixed before transferring to sample vials for analysis. Standard calibration range was up to 8 mg/L. The coefficients of variation for measurement of two internal control samples were 2.44%, and 1.57%, respectively, for within-day precision ($n = 14$); 1.45% and 1.66% for day-to-day precision ($n = 3$). Rabbit liver samples (200 mg) were digested with 4 ml concentrated HNO_3 and 1 ml H_2O_2 using microwave oven acid digestion method. The digested samples were well-mixed and further diluted 100-times with deionized water [13]. Standard calibration range covered up to 12 mg/L. The coefficients of variation for measurement of two internal control samples were 3.16% and 2.56%, respectively, for within-day precision ($n = 8$).

Serum and liver lipid analyses

Serum cholesterol levels were measured by routine clinical reagents from Thermo Scientific (Infinity™ Cholesterol Cat#13421, Louisville, CO). Serum and liver lipids were extracted, hydrolysed and analysed using gas chromatography-mass spectrometry (GC-MS) from frozen liver (50 mg), as described in detail previously [6,14,15]. In brief, lipid was extracted from liver homogenates using organic solvent (chloroform/methanol 2:1 v/v + 0.005% butylated hydroxytoluene (BHT)) (VWR International Ltd, Hunter Boulevard, UK) and dried under a stream of N_2. After addition of heavy isotopic standards of F_2-isoprostanes and cholesterol oxidation products (COPs), samples were reconstituted in 1 ml PBS and 1 ml KOH (1 M in methanol) and hydrolysed overnight at 23°C in the dark under an argon atmosphere. Solid phase extraction was carried out using 60 mg MAX (mixed ion exchange, Waters) columns. After elution of COPs followed by elution of F_2-isoprostanes, extracts were dried under N_2 gas, derivatized and analysed by an Agilent 5975 mass selective detector interfaced with an Agilent 5890II gas chromatograph. Selected-ion monitoring was performed to monitor ions selected from each compound's mass spectrum in order to optimize sensitivity and specificity. Quantification of F_2-isoprostanes and COPs was carried out by relating the total peak area of each analyte with their heavy isotopic internal standard peak except for the 5,6-cholesterol epoxides which used 7 beta hydroxycholesterol d_7.

Liver haemotoxylin and eosin, Sudan red and Perl's histochemistry

Liver specimens were immersion fixed in 4% paraformaldehyde (BDH, Hunter Boulevard) in 0.1 M phosphate buffer. A portion of this tissue was

Table I. Serum cholesterol levels in normal and cholesterol fed rabbits, at 0, 4 and 8 weeks after the start of high cholesterol diet in the cholesterol fed rabbits or an identical diet without cholesterol in the normal rabbits. A marked increase in serum cholesterol level is found at 4 and 8 weeks in the cholesterol-fed rabbits. Significant increases were observed in serum cholesterol in the 4- and 8-week cholesterol-fed rabbits, compared to normal controls.

	Normal rabbits (mg/dl, $M \pm$SD)			Cholesterol-fed rabbits (mg/dl, $M \pm$SD)		
Lipid	0 weeks	4 weeks	8 weeks	0 weeks	4 weeks	8 weeks
Serum cholesterol	37 ± 10	44 ± 16	137 ± 57	51 ± 20	2193 ± 1044*	1800 ± 262*

* $p < 0.05$ by Student's *t*-test.

processed for paraffin wax sectioning and staining with haemotoxylin and eosin (Thermo Fisher Scientific Inc., Waltham, MA) for routine examination of liver cytoarchitecture. Another portion was processed for frozen sectioning and Sudan red histochemistry to demonstrate the presence of lipids. A third portion was sectioned at 100 μm thickness using a Vibratome and the sections processed for Perls' stain to detect iron or immunohistochemistry. Perl's stain was carried out by immersing the sections in a potassium ferrocyanide mixture (containing 1 part of 10% v/v aqueous potassium ferrocyanide and 0.5 part of 10% v/v hydrochloric acid) (Merck KGaA, Darmstadt, Germany) for 30 min, followed by washing with distilled water and 3,3,-diaminobenzidine tetrahydrochloride (DAB) (Sigma, St. Louis, MI) enhancement as described previously [16]. Sections intended for immunohistochemistry were incubated overnight with affinity purified goat polyclonal antibodies to transferrin receptor-1 (1:250), divalent metal transporter-1 (DMT1) (1:250), ceruloplasmin (1:250) and melanotransferrin (1:250) (all from Santa Cruz Biotechnology, Santa Cruz, CA) or mouse monoclonal antibodies to 4-hydroxynonenal (clone HNE-J2, specific for 4-HNE-His/Lys/Cys adducts, Japan Institute for the Control of Aging, Fukuroi, Japan, 1:200) and CD68 (KAL-KT015, Cosmo Bio Ltd, 1:100). The sections were washed in three changes of PBS and incubated for 1 h at room temperature in a 1:200 dilution of biotinylated rabbit anti-goat IgG or horse anti-mouse antibody (Vector Laboratories, Burlingame, CA). This was followed by three changes of phosphate buffered saline (PBS) and incubation for 1 h at room temperature with an avidin–biotinylated horseradish peroxidase complex (Vector Laboratories). The reaction was visualized by treatment for 5 min in DAB solution in Tris buffered saline (TBS) containing 0.05% hydrogen peroxide. Control sections were incubated with PBS or melanotransferrin antigen-absorbed antibody (0.8 μg/ml of melanotransferrin immununizing antigen to 1:250 of anti-melanotransferrin antibody, Santa Cruz Biotechnology, Santa Cruz, CA) instead of primary antibody. They showed absence of labelling (data not shown).

Some of the Perl's stained or immunostained sections were mounted on glass slides, lightly counterstained with methyl green, dehydrated and coverslipped. The number of iron or melanotransferrin positive cells was counted 'blind' on coded slides at 200 × magnification from each animal and expressed as number of positive cells/unit area. Possible significant differences between the cholesterol fed and normal rabbits were analysed using Student's *t*-test. The remaining sections were processed for electron microscopy. These were osmicated, dehydrated in an

Table II. Cholesterol and oxidized lipid levels in the liver of normal and hypercholesterolemic rabbits, at 8 weeks after the start of high cholesterol diet in the cholesterol-fed rabbits or an identical diet without cholesterol in the normal rabbits. Significant increases were observed in cholesterol and oxidized lipid biomarkers in the liver of cholesterol-fed rabbits, compared to normal controls. Significant increases were also observed in the level of the COPs, 7 beta hydroxycholesterol, 7 ketocholesterol and cholesterol 5,6, alpha epoxide after normalizing to the level of cholesterol in liver tissue, in the cholesterol-fed rabbits.

Lipid	Normal rabbits (ng/mg tissue, $M \pm$SD)	8-Week cholesterol-fed rabbits (ng/mg tissue, $M \pm$SD)	Normal rabbits COP (μmol)/cholesterol (mol) ($M \pm$SD)	8-Week cholesterol-fed rabbits COP (μmol)/cholesterol (mol) ($M \pm$SD)
Cholesterol	2500 ± 300	17 300 ± 1500*		
7 beta Hydroxycholesterol	0.5 ± 0.2	7.2 ± 1.1*	204 ± 70	405 ± 93*
7 Ketocholesterol	0.4 ± 0.1	5.8 ± 1.7*	156 ± 37	325 ± 107*
Cholesterol 5,6 beta epoxide	0.3 ± 0.1	2.0 ± 0.7*	117 ± 49	116 ± 45
Cholesterol 5,6 alpha epoxide	0.07 ± 0.03	1.8 ± 0.7*	27 ± 14	100 ± 38*
F_2-isoprostanes	1.3 ± 0.3	2.1 ± 0.5*		

* $p < 0.05$ by Student's *t*-test.

ascending series of ethanol and acetone and embedded in Araldite (all are from Electron Microscopy Sciences, Hatfield, PA). Ultrathin sections were obtained from the first 5 μm of the sections, mounted on copper grids coated with Formvar and stained with lead citrate. They were viewed using a Philips EM208 electron microscope.

Results

Serum and liver lipid analyses

A significant increase in total cholesterol was detected in the serum of the 4- and 8-week cholesterol-fed rabbits, compared to those on normal diet (Table I). Significant increases were also observed in the level of the cholesterol in the liver and of the cholesterol oxidation products (COPs), 7 beta hydroxycholesterol, 7 ketocholesterol and cholesterol 5,6, alpha epoxide. The differences persisted after normalizing to the level of cholesterol in liver tissue, in the cholesterol-fed rabbits (Table II). The above oxysterols are generally considered to be produced by chemical reaction of cholesterol with reactive oxygen species, although some evidence suggests that cholesterol 5,6, alpha epoxide can also be formed through the action of microsomal enzymes [17].

Serum and liver iron analyses

No significant difference in iron levels was detected in the serum of cholesterol-fed rabbits (1.89 ± 0.68 mg/L) compared to those on normal diet (1.81 ± 0.73 mg/L) ($p = 0.856$). A trend to an increase in iron levels, but non-significant, was observed in liver homogenates of cholesterol-fed rabbits (281 ± 99 ng/mg), compared to normal controls (250 ± 42 ng/mg) ($p = 0.586$).

Light microscopy

Haemotoxylin and eosin, Sudan red and Perl's histochemistry. In contrast to the generally uniform

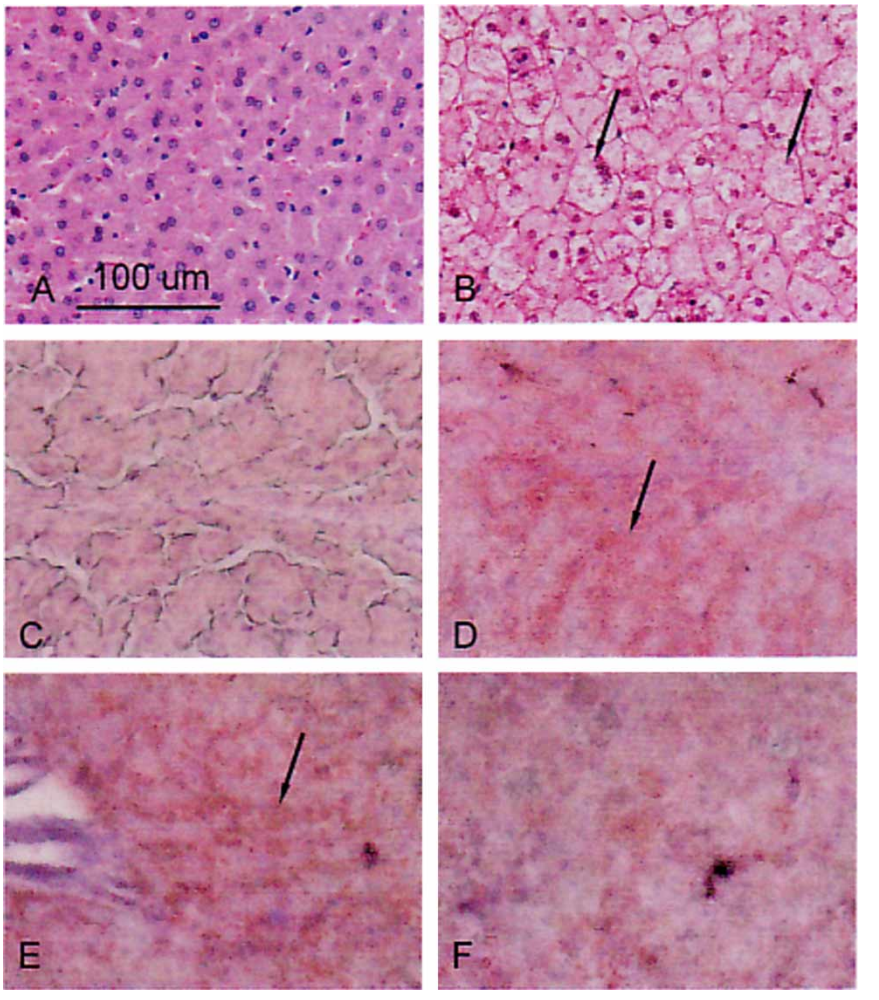

Figure 1. Haemotoxylin and eosin stained sections from a normal rabbit (A) and a hypercholesterolemic rabbit (B). Increased amount of clear cytoplasm is present in the hepatocytes in the hypercholesterolemic rabbit (arrows). (C) Sudan red stained sections from a normal rabbit showing little staining. (D, E) Zone I of liver acinus from a hypercholesterolemic rabbit showing increase in number of lipid droplets (arrows). (F) Centre of a liver lobule in a hypercholesterolemic rabbit, showing fewer lipid droplets compared to the periphery (D, E). Scale = 100 μm.

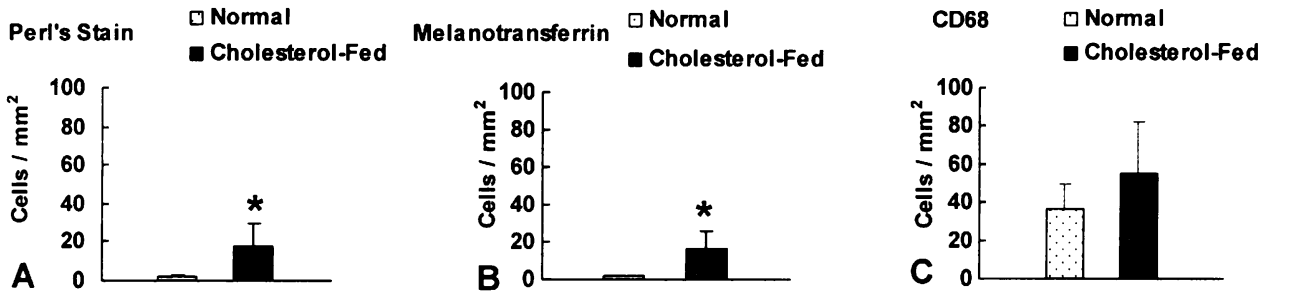

Figure 2. Number of Perl's stained (A), melanotransferrin immunostained (B) or CD68 immunostained (C) cells per mm^2 in the liver of normal and hypercholesterolemic rabbits. Significantly greater number of Perl's stained or melanotransferrin-immunostained cells identified at electron microscopy as putative macrophages, but non-significant trend to an increase in number of CD68 positive total macrophages (including endogenous Kupffer cells and possibly exogenous blood borne macrophages) was observed in the liver of cholesterol-fed rabbits, compared to normal controls. Asterisks indicate significant difference by *t*-test ($p < 0.05$).

appearance of the cytoplasm of normal liver cells (Figure 1A), a large number of vacuoles were observed in the cytoplasm of hepatocytes of cholesterol-fed rabbits (Figure 1B). Sudan red stained sections showed few lipid droplets in hepatocytes of the normal rabbit (Figure 1C), but increased accumulation of lipid droplets (red granules) in hepatocytes of the cholesterol-fed rabbits. The droplets appeared to be denser in hepatocytes at zone I of liver acinus (Figure 1D and E) than those in the centre (Figure 1F).

Perl's stained sections showed only occasional stained cells in the liver of normal rabbits, but significantly greater numbers of cells in the hypercholesterolemic rabbits (Figure 2A, 3A and B). The cells mostly present around vessels of the portal triad (tract), along the interlobular arterioles and venules and in zone I of the liver acinus (periportal region of the classic hepatic lobule) (Figure 3C). Few cells were observed along liver sinusoids or zones II and III of the liver acinus (mid-zone and pericentral region of the classic hepatic lobule). The Perl's stained cells had irregular outlines (Figure 3D) and were putatively identified as macrophages that have infiltrated from the bloodstream into the liver parenchyma.

Immunohistochemistry. Immunoreactivity to transferrin receptor, divalent metal transporter-1 and ceruloplasmin expression remained at basal levels in the hypercholesterolemic rabbits (data not shown). In contrast, a marked increase in melanotransferrin labelling was observed after cholesterol feeding (Figure 2B, 4A and B). The labelled cells were present around vessels of the portal triad, interlobular arterioles and venules and in zone I of the liver acinus

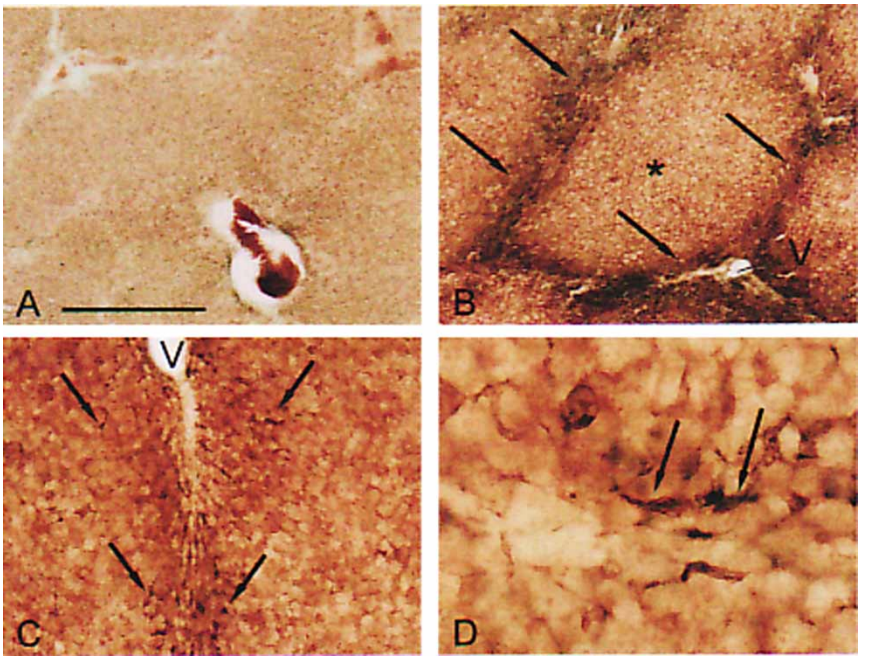

Figure 3. (A) Perl's stained section of the liver of a normal rabbit, showing little staining. (B) Perl's stained section from a hypercholesterolemic rabbit, showing increased staining in zone I of liver acinus (arrows) and around perilobular vessels (V). In contrast, less staining is present in the centre of the lobule (asterisk). (C, D) Higher magnification of zone I of liver acinus showing iron positive cells. These have irregular cell outlines and features of macrophages (arrows). Scale: (A, B) = 200 μm, (C, D) = 33 μm.

(Figure 4C) and had features of macrophages (Figure 4D).

Little or no staining to 4-HNE was observed in the liver of normal rabbits (Figure 4E). In comparison, moderately dense staining was observed around the portal triad and zone I of the liver acinus in hypercholesterolemic rabbits (Figure 4F). Label was present in hepatocytes.

A non-significant trend to an increase in number of CD68 positive macrophages (including endogenous Kupffer cells and possibly exogenous blood borne macrophages) was observed in the liver of cholesterol-fed rabbits, compared to normal controls ($p = 0.104$; Figure 2C).

Electron microscopy

Electron microscopy confirmed that the Perl's stained cells had large numbers of vacuoles and dense bodies or lysosomes and features of macrophages (Figure 5A). Cells with very similar features were immunolabelled for melanotransferrin (Figure 5B). Reaction product was present on the cell membrane of the labelled cells, consistent with the membrane-bound form of the protein (Figure 5C). Both Perls' stain and melanotransferrin stained cells were found in the liver parenchyma around blood vessels. Many cells were observed with part of a cytoplasmic process in contact with a blood vessel and appeared to be infiltrating from the vessels (Figure 5A).

Discussion

The present study was carried out to elucidate possible changes in iron and iron handling proteins in the liver of cholesterol-fed rabbits. The latter is a well-known model for studying changes after hypercholesterolemia. The level of iron was first studied in gross specimens of the rabbit liver, using AAS. A

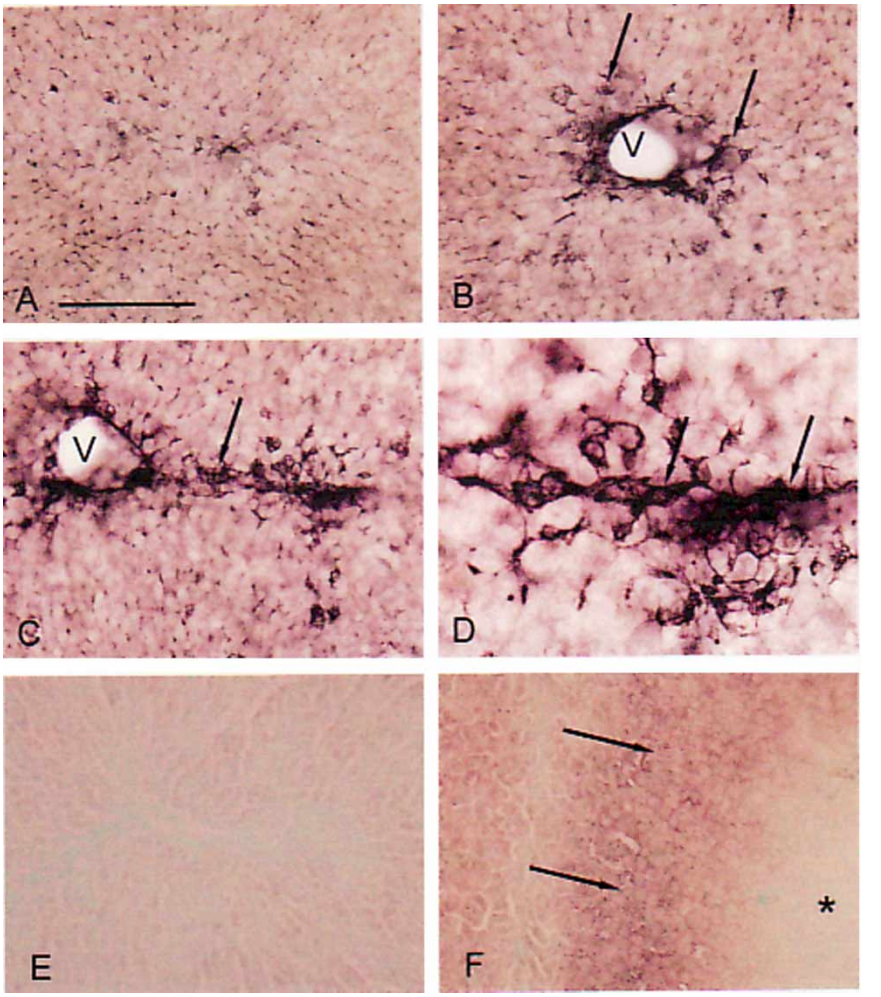

Figure 4. (A) Melanotransferrin-stained section of the liver of a normal rabbit, showing little staining. (B, C) Melanotransferrin-stained section of a hypercholesterolemic rabbit showing many labelled cells (arrows) associated with perilobular vessels (V). (D) Higher magnification of melanotransferrin-positive cells. These have irregular cell outlines and features of macrophages (arrows). (E) HNE immunostained section from a normal rabbit showing very little or no staining. (F) HNE immunostained section from a hypercholesterolemic rabbit, showing increased staining in zone I of liver acinus (arrows). In contrast, little staining is present in the centre of the lobule (asterisk). Scale: (A, B) = 200 μm, (C, E, F) = 100 μm, (D) = 33 μm.

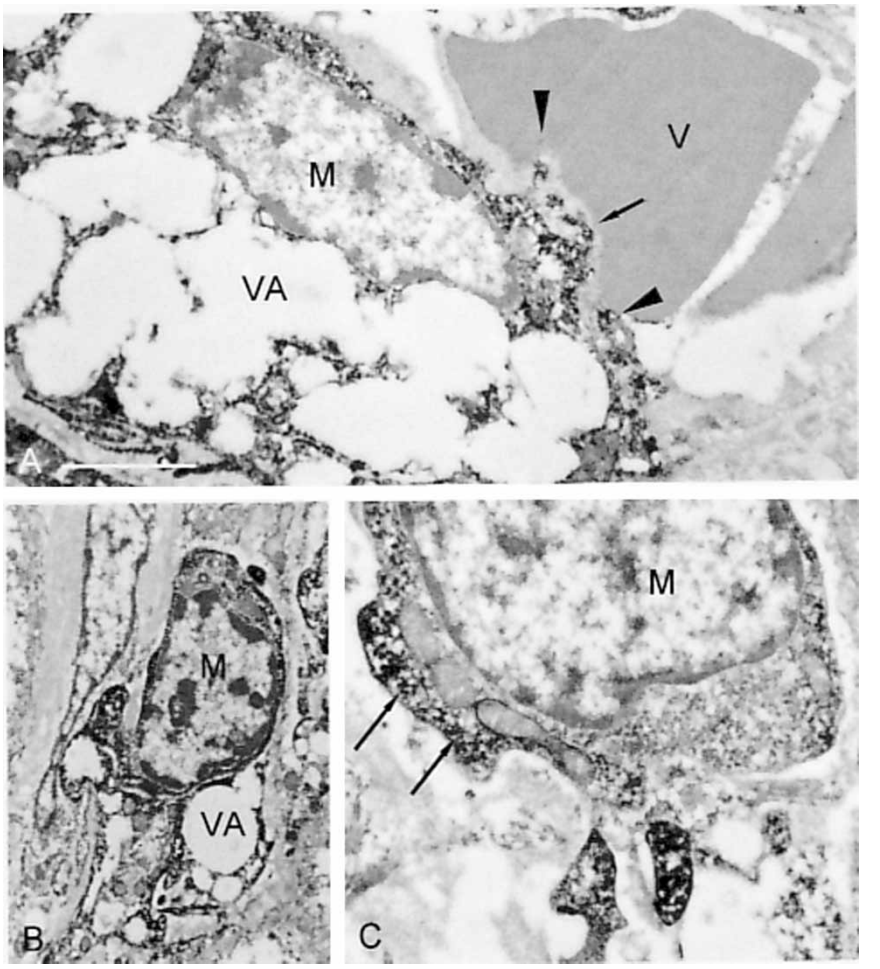

Figure 5. (A) Electron micrographs of a Perl's stained, iron-containing cell (M) in the liver of cholesterol-fed rabbits. The cell body has an irregular outline, dense heterochromatin in the nucleus and large number of vacuoles (VA) characteristic of macrophages. A portion of the cytoplasm (arrow) appears to be passing through a breach in the vessel wall (arrowheads) and the cell is putatively identified as a blood macrophage that is infiltrating from the vessel into the liver parenchyma. V: lumen of vessel. (B, C) Electron micrographs of melanotransferrin-positive cells (M) in the liver of cholesterol-fed rabbits. These have very similar features to the Perl's stained cells including nuclei with dense heterochromatin and vacuoles in the cytoplasm (VA). Melanotransferrin label is present on the cell membrane (arrows in C), consistent with the membrane bound form of the iron protein. Scale: (A, C) = 3 μm, (B) = 5 μm.

trend to an increase, but non-significant, in iron level was observed at the macroscopic level. This is consistent with previous reports, of no significant changes in iron levels at the macroscopic level, in the liver of cholesterol-fed rabbits [18] or Watanabe Heritable Hyperlipidemic rabbits [19]. Possible changes in iron were then examined at a histological level in the liver, utilizing the well-established Perl's stain method. The results showed a significant increase in the number of iron-positive macrophages around vessels of the portal triad, perilobular vessels and zone I of the liver acinus in rabbits that were fed with a high cholesterol diet. They indicate an increase in iron at a microscopic level, even before significant increase is detectable at the organ level.

Immunohistochemical analyses showed that the level of the metal transport proteins, transferrin receptor-1, divalent metal transporter-1 and ceruloplasmin remained at baseline levels in the hypercholesterolemic rabbits. In contrast, a marked increase in melanotransferrin expression was observed in the liver of the hypercholesterolemic rabbits. The distribution of the melanotransferrin positive cells was very similar to that of Perl's stained sections, i.e. labelled cells were present around blood vessels of the portal triad, perilobular vessels and in zone I of the liver acinus. Both Perl's stained and melanotransferrin positive cells had ultrastructural features of macrophages, but were not found along liver sinusoids. This suggests that they were not resident Kupffer cells, but blood monocytes that have infiltrated into the liver parenchyma. Melanotransferrin could be important for cell proliferation or migration of cells [20,21] and might be important for entry of iron containing macrophages into the liver during hypercholesterolemia. Mice deficient in melanotransferrin show reduced expression of genes involved in proliferation and melanoma cells with decreased melanotransferrin expression showed reduced tumour growth [20,21]. Increased melanotransferrin-positive microglia/macrophages

have also been observed in the brains of Alzheimer's disease patients [22].

Increased lipid peroxidation, as evidenced by elevated isoprostane and carbonyl levels, has previously been reported in the liver of mice on a high fat diet [23] or TBARS measurement (a much less-robust biomarker) in the hypercholesterolemic rabbit [24]. Free cholesterol loading, but not free fatty acids or triglycerides, causes depletion of glutathione in hepatocytes and sensitizes these cells to tumour necrosis factor and Fas-induced steatohepatitis [25]. In this study, we demonstrated an increase in the arachidonic acid peroxidation product F_2-isoprostanes in the liver and significant increases in the level of several COPs, indicating that increased oxidative stress leads to disproportionately increased oxidation of cholesterol, in the liver of the cholesterol-fed rabbits. We also showed greater accumulation of lipids by Sudan red labelling in hepatocytes in zone I than in zone II and III of the liver acinus. The increase in lipids in zone I coincided with the increase in iron and 4-HNE staining in the same zone and suggests that there is a close correlation between the increase in lipids and iron and the occurence of lipid peroxidation in vulnerable parts (zone I) of the liver acinus in hypercholesterolemia. One possibility is that there is microvascular damage during hypercholesterolemia, leading to increased influx of lipids and iron/infiltration of iron-rich macrophages, which in turn cause increased oxidative stress in the adjacent tissues [12,26].

It has to be noted that the values of serum cholesterol in the present model are much higher than observed in humans. Nevertheless, increased insulin resistance and cholesterol to HDL ratios have been found in patients with non-alcoholic steatohepatitis compared to controls [27], suggesting that hypercholesterolemia may indeed predispose to liver damage in human patients. Further work is necessary to study endothelial dysfunction induced by hypercholesterolemia and whether lipid and iron accumulation and increased oxidative stress is a common feature of microvasculatures in hypercholesterolemia.

Acknowledgements

We are grateful to the BMRC Singapore for support through Grant 04/1/21/19/328. We thank Professer Yoke-Sun Lee for valuable discussion.

***Declaration of interest*:** The authors report no conflicts of interest. The authors alone are responsible for the content and writing of the paper.

References

[1] Halliwell B, Gutteridge JMC. Free radicals in biology and medicine. 4th ed. Oxford: Elsevier; 2007.

[2] Lee FY, Lee TS, Pan CC, Huang AL, Chau LY. Colocalization of iron and ceroid in human atherosclerotic lesions. Atherosclerosis 1998;138:281–288.

[3] Yuan XM. Apoptotic macrophage-derived foam cells of human atheromas are rich in iron and ferritin, suggesting iron-catalysed reactions to be involved in apoptosis. Free Radic Res 1999;30:221–231.

[4] Araujo JA, Romano EL, Brito BE, Parthe V, Romano M, Bracho M, Montano RF, Cardier J. Iron overload augments the development of atherosclerotic lesions in rabbits. Arterioscler Thromb Vasc Biol 1995;15:1172–1180.

[5] Ren M, Rajendran R, Pan N, Tan BK-H, Ong WY, Watt F, Halliwell B. The iron chelator desferrioxamine inhibits atherosclerotic lesion development and decreases lesion iron concentrations in the cholesterol-fed rabbit. Free Radic Biol Med 2005;38:1206–1211.

[6] Jenner A, Ren M, Rajendran R, Ning P, Tan BK-H, Watt F, Halliwell B. Zinc supplementation inhibits lipid peroxidation and the development of atherosclerosis in rabbits fed a high cholesterol diet. Free Radic Biol Med 2007;42:559–566.

[7] Lee TS, Shiao MS, Pan CC, Chau LY. Iron-deficient diet reduces atherosclerotic lesions in apoE-deficient mice. Circulation 1999;99:1222–1229.

[8] Ong WY, Tan B, Pan N, Jenner A, Whiteman M, Ong CN, Watt F, Halliwell B. Increased iron staining in the cerebral cortex of cholesterol fed rabbits. Mech Ageing Dev 2004;125:305–313.

[9] Ong WY, Halliwell B. Iron, atherosclerosis, and neurodegeneration: a key role for cholesterol in promoting iron-dependent oxidative damage? Ann N Y Acad Sci 2004;1012:51–64.

[10] Langheinrich AC, Michniewicz A, Bohle RM, Ritman EL. Vasa vasorum neovascularization and lesion distribution among different vascular beds in ApoE $^{-/-}$/LDL$^{-/-}$ double knockout mice. Atherosclerosis 2007;191:73–81.

[11] Gossl M, Beighley PE, Malyar NM, Ritman EL. Role of vasa vasorum in transendothelial solute transport in the coronary vessel wall: a study with cryostatic micro-CT. Am J Physiol Heart Circ Physiol 2004;287:H2346–H2351.

[12] Ritman EL, Lerman A. The dynamic vasa vasorum. Cardiovasc Res 2007;75:649–658.

[13] Araújo GC, Nogueira AR, Nóbrega JA. Single vessel procedure for acid-vapour partial digestion in a focused microwave: Fe and Co determination in biological samples by ETAAS. Analyst 2000;125:1861–1864.

[14] Lee CY, Jenner AM, Halliwell B. Rapid preparation of human urine and plasma samples for analysis of F2-isoprostanes by gas chromatography-mass spectrometry. Biochem Biophys Res Commun 2004;320:696–702.

[15] He X, Jenner AM, Ong WY, Farooqui AA, Patel SC. Lovastatin modulates increased cholesterol and oxysterol levels and has a neuroprotective effect on rat hippocampal neurons after kainate injury. J Neuropathol Exp Neurol 2006;65:652–663.

[16] Hill JM, Switzer RC 3rd. The regional distribution and cellular localization of iron in the rat brain. Neuroscience 1984;11:595–603.

[17] Schroepfer GJ. Oxysterols: modulators of cholesterol metabolism and other processes. Physiol Rev 1990;80:361–554 .

[18] Klevay LM. Dietary cholesterol lowers liver copper in rabbits. Biol Trace Elem Res 1988;16:51–57.

[19] Allain P, Krari N, Chaleil D, Balanant Y, Bled F, Girault M. The distribution of elements in the tissues of Watanabe heritable hyperlipidemic rabbits. Biol Trace Elem Res 1989;19:153–160.

[20] Dunn LL, Sekyere EO, Rahmanto YS, Richardson DR. The function of melanotransferrin: a role in melanoma cell proliferation and tumorigenesis. Carcinogenesis 2006;27:2157–2169.

[21] Bertrand Y, Demeule M, Michaud-Levesque J, Béliveau R. Melanotransferrin induces human melanoma SK-Mel-28 cell invasion *in vivo*. Biochem Biophys Res Commun 2007;353:418–423.
[22] Yamada T, Tsujioka Y, Taguchi J, Takahashi M, Tsuboi Y, Moroob I, Yang J, Jefferies WA. Melanotransferrin is produced by senile plaque-associated reactive microglia in Alzheimer's disease. Brain Res 1999;845:1–5.
[23] Ding T, Yao Y, Pratico D. Increase in peripheral oxidative stress during hypercholesterolemia is not reflected in the central nervous system: evidence from two mouse models. Neurochem Int 2005;46:435–439.
[24] Kang MH, Kawai Y, Naito M, Osawa T. Dietary defatted sesame flour decreases susceptibility to oxidative stress in hypercholesterolemic rabbits. J Nutr 1999;129:1885–1890.
[25] Marí M, Caballero F, Colell A, Morales A. Caballeria J, Fernandez A, Enrich C, Fernandez-Checa JC, García-Ruiz C. Mitochondrial free cholesterol loading sensitizes to TNF- and Fas-mediated steatohepatitis. Cell Metab 2006;4:185–198.
[26] Ghribi O, Golovko MY, Larsen B, Schrag M, Murphy EJ. Deposition of iron and beta-amyloid plaques is associated with cortical cellular damage in rabbits fed with long-term cholesterol-enriched diets. J Neurochem 2006;99:438–449.
[27] Bookman ID, Pham J, Guindi M, Heathcote EJ. Distinguishing nonalcoholic steatohepatitis from fatty liver: serum-free fatty acids, insulin resistance and serum lipoproteins. Liver Int 2006;26:566–571.

This paper was first published online on iFirst on 31 January 2009.